International Dairy Journal 132 (2022) 105399

Contents lists available at ScienceDirect

International Dairy Journal

journal homepage: www.elsevier.com/locate/idairyj

Whey protein microgels for stabilisation of foams

Jenna Lee, Elaine Duggan*

Eco-Innovation Research Group, Department of Science in School of Science and Computing, Waterford Institute of Technology, Waterford, Ireland

ARTICLE INFO

Article history:
Received 17 November 2021
Received in revised form
4 April 2022
Accepted 10 April 2022
Available online 26 April 2022

ABSTRACT

Rheological, foaming and foam textural properties of whey protein isolate (WPI) microgels formed via cold-set gelation were investigated and compared with those of native WPI foams. The effect of $CaCl_2$ concentration and cross-linking time on microgel formation was studied assessing particle size, rheology and foamability. Foams, produced by mechanical whipping, were assessed by overrun, stability and texture. WPI had lower viscosity than the microgels, producing foams with greater overrun. For microgels, higher concentrations of $CaCl_2$ formed smaller particles and decreased microgel viscosity, causing higher overrun. Increasing cross-linking time from 0 to 24 h significantly ($P < 0.05$) increased G′ and G″ of the microgels, resulting in decreased overrun. Native WPI foams drained within 60 min. In contrast, negligible amounts of liquid drained from microgel foams, which remained stable for >2 years. This demonstrates that WPI microgels can be used as a novel functional application for creating ultra-stable foams for use in the food industry.

1. Introduction

Foams consist of air bubbles distributed throughout a continuous aqueous phase separated by films called lamellae. The surface tension between the air/water interface is five times larger than that between water and oil (Lazidis et al., 2016). According to Hill and Eastoe (2017) the surface tension phenomenon is due to the imbalance of attractive intermolecular interactions at the surface of the liquid. Additional energy is required to create the interface between air and water which is attributed to the surface tension. Therefore, foams require amphiphilic entities to adsorb at the surface to reduce the tension.

Pickering stabilisation has been found to protect bubbles against coalescence, whereby closely packed solid particles adsorb at the interface forming a monolayer around a bubble. When two bubbles come in to close proximity, the particle layer prevents coalescence, thus stabilising the bubble (Dickinson, 2017). In the past, most of the research has focused on using inorganic particles for stabilisation, such as silica particles (Lam, Velikov, & Velev, 2014). However, inorganic particles have limited relevance when it comes to an application requiring biocompatibility and biodegradability thus making them unsuitable for food foams (Lam et al., 2014).

In recent years there has been increased interest in the use of microgels for foam stability as they are deformable and versatile (Schmitt, Destribats, & Backov, 2014). These microgel particles are soft porous particles made from polymers such as proteins or polysaccharides. Studies in recent years have shown that microgels can lead to dispersions being far more stable than those produced by surfactants (Asghari, Norton, Mills, Sadd, & Spyropoulos, 2016; Ellis, Mills, Norton, & Norton-Welch, 2019; Lazidis et al., 2016; Li, Murray, Yang, & Sarkar, 2020a; Li, Yang, Murray, & Sarkar, 2020b). The reason for this is because the energy of desorption is greater for a particle than for a smaller surfactant (Cox, Aldred, & Russell, 2009).

Food proteins are defined as those that are non-toxic, easily digestible, available in abundance, nutritionally adequate and sustainable agriculturally (Damodaran, Perkin, & Fennema, 2007). Whey proteins are known for their high nutritional value and functional properties and are widely used in the food industry for nutritional purposes such as prevention of cancers (Gill & Cross, 2000), antioxidant activity (Bayram, Pekmez, Arda, & Yalçin, 2008) and use for weight management due to the satiety effect of whey proteins (Weigle et al., 2005). Many proteins are insoluble at their isoelectric point (pI), making it difficult to use them in solution around this pH. However, whey proteins are soluble at their pI and can be utilised, making them applicable for addition into acidic beverages such as fruit juices or soft drinks (Ron, Zimet, Bargarum, & Livney, 2010; Ustunol, 2014). Whey proteins are also utilised as functional ingredients in foods due to their ability to form gels and

* Corresponding author.
E-mail address: eduggan@wit.ie (E. Duggan).

https://doi.org/10.1016/j.idairyj.2022.105399

emulsions and can act as delivery vehicles for bioactive compounds (Abbasi, Emam-Djomeh, Mousavi, & Davoodi, 2014; Bryant & McClements, 2000; Lazidis et al., 2016; Lee & Duggan, 2022; Li et al., 2022; Madadlou et al., 2020; Tan, Liu, Zhou, Mundo, & McClements, 2019).

In this study, cold-set gelation was used to make microgel particles. This involves heating a solution of native protein while controlling pH and protein concentration; this causes partial protein unfolding that exposes thiol groups (Kuhn, Cavallieri, & da Cunha, 2010). Reducing the electrostatic repulsion between the protein aggregates will initiate cold-set gelation. This is done by increasing the mineral content or adjusting the pH of the solution (Bryant & McClements, 2000).

There are two main ways, mechanistically speaking, for microgel particles to function as stabilising agents and foams. The particles can create a gel-like network within the spaces amongst the gas bubbles when they are present at high concentrations in the bulk continuous phase. On the other hand, the particles can generate a particle-loaded surface layer by becoming directly attached to the air–water interface, which works to protect the bubbles (Dickinson, 2017). A combination of these mechanisms can be present in a multi-phase food system as some particles may be dispersed in the bulk phase while others are located within the thin liquid film.

The objective of this study was to investigate the potential of whey protein microgel particles to produce and stabilise foamed systems for prolonged periods. The particle stabilised foams were compared with foams produced with native whey protein.

2. Materials and methods

2.1. Materials

Whey protein isolate (WPI) (BiPro, 97.8%, w/w, total protein) was purchased from Agropur Inc. (Minnesota, USA). Sodium chloride (NaCl), calcium chloride ($CaCl_2$) and sodium azide were purchased from Lennox (Dublin, Ireland). 8-Anilinonaphthalene-1-sulfonic acid (ANS) and 5,5-dithiobis (2-nitrobenzoic acid) (DTNB, Ellman's Reagent) were purchased from Sigma–Aldrich (Wicklow, Ireland). SeeBlue Plus2 pre-stained protein standard and MES SDS running buffer and InstantBlue Coomassie Stain were purchased from ThermoFisher Scientific (Dublin, Ireland).

2.2. Preparation of whey protein isolate solution and microgels

Whey protein isolate was prepared by dissolving the powder in deionised water at room temperature using a magnetic stirrer to make a 10% (w/w) protein solution. Sodium azide was added (0.02%) to prevent microbial growth. The rehydrated samples were kept in the refrigerator at 4 °C overnight to fully hydrate.

For creating the microgels, cold-set gelation was used. The protein solution was pre-heated in a water bath at 80 °C for 30 min followed by cooling on ice to room temperature. Calcium chloride at concentrations of 0.02, 0.05 and 0.1 M was used to cross-link the denatured protein samples (pH 6.8) to form microgels. All samples were left to cross-link at 4 °C for 24 h. Once the optimum $CaCl_2$ concentration was chosen on the basis of optimum foam overrun and stability, the effect of cross-linking time was analysed at 0 or 24 h.

2.3. Particle size

Particle size distributions were determined using static light scattering. A Malvern Mastersizer Hydro 2000S (Malvern Instruments, Royston, UK) was used to obtain the surface weighted mean, $d_{3,2}$. Samples were diluted in distilled water to avoid multiple scattering. A refractive index of 1.33 and 1.456 was used for water and whey protein, respectively. All size measurements were carried out in three replicates.

2.4. Sodium dodecyl sulphate polyacrylamide gel electrophoresis

The protein fractions were analysed by sodium dodecyl sulphate polyacrylamide gel electrophoresis (SDS-PAGE). The protein solutions were diluted to a final protein concentration of ~0.2%. Samples were prepared with an SDS-PAGE buffer under reducing conditions (0.125 M Tris–HCl pH 6.8, 4% SDS, 20% glycerol, bromophenol, 10% β-mercaptoethanol) or non-reducing conditions (without β-mercaptoethanol). Mixture of sample and sample buffer (1:1, v/v) was heated to 100 °C for 5 min and cooled on ice. The microgel samples were centrifuged at 10,000 × *g* for 10 min. Five μL of each sample were loaded into Bolt Bis-Tris gel (ThermoFisher Scientific, Dublin, Ireland) consisting of a 4–12% gradient capable of separating proteins up to 260 kDa. Molecular masses of the protein bands were estimated by means of the protein marker (SeeBlue Plus2 Prestained protein standard). The running buffer, MES SDS (20×) was diluted to 1× and the migration was performed at a constant voltage of 200 V for 22 min. Gels were stained with InstantBlue Coomassie Stain. Images of the gels were captured using the iBright FL1000 Imaging system (ThermoFisher Scientific).

2.5. Determination of accessible sulphydryl content

The concentration of free sulphydryl groups were measured according to the Ellman's Reagent protocol (Thermoscientific, 2020) using Ellman's reagent. The effect of cross-linking time of WPI with 0.1 M $CaCl_2$ on free sulphydryl content was analysed. Protein solutions were diluted (1:5) with distilled water and 500 μL of the protein sample was mixed with 5 mL reaction buffer (0.1 M sodium phosphate, 1 mM EDTA, pH 8.0) and 100 μL Ellman's reagent. Samples were left to incubate for 15 min at room temperature. Samples were then centrifuged at 4000 × *g* for 15 min and their absorbance at 412 nm were measured using UV–vis spectrophotometer. The concentration of accessible SH was determined using a standard curve (0.25–1.5 mM cysteine).

2.6. Surface hydrophobicity

The surface hydrophobicity of samples was determined using the fluorescence probe, 8-anilinonaphthalene-1-sulfonic acid (ANS) (8 mM in 0.01 M phosphate buffer, pH 8.0) (Alavi, Tian, Chen, & Emam-Djomeh, 2020) with slight modification. A series of protein solutions with concentrations from 0.0025 to 0.02% was prepared by diluting native, heat denatured and WPI microgel solutions with 0.01 M phosphate buffer, pH 8. Forty microlitres of ANS solution was added to 4 mL of each protein solution and the fluorescence intensity was recorded with a spectrophotometer (Cary Eclipse fluorescent spectrophotometer, Agilent, Middelburg, The Netherlands) at the excitation and emission wavelengths of 365 and 484 nm respectively. A control sample containing phosphate buffer without WPI was mixed with ANS, the fluorescent intensity of the control was used to estimate the relative fluorescent intensity (RFI). The RFI was calculated for each sample by dividing the fluorescent intensity of the sample by the fluorescent intensity of the control. RFI was plotted against the protein concentrations and the slope (H_0) of the line for each sample was taken as the surface hydrophobicity.

2.7. Analysis of rheological properties

Viscosity and rheological measurements were performed in a shear stress controlled rotational rheometer (AR-G2 rheometer, TA instruments, New Castle, DE, USA). A parallel plate geometry with a diameter of 40 mm with a gap of 500 μm was used. Viscosity values were measured at a shear rate of 100 s^{-1} at 20 °C.

A strain-controlled frequency sweep (0.01–10 Hz) at a strain (0.2%) within the linear viscoelastic region (LVR) was applied. The LVR was determined by an amplitude sweep performed beforehand for the same sample. Time sweeps (120 min) were also carried out at 0.2% strain and 1 Hz. The storage (G′) and loss modulus (G″) were recorded. All measurements were carried out in triplicate.

2.8. Preparation of foams

Foams were prepared using a standard kitchen hand blender (Kenwood) at speed 3 for 5 or 10 min. Samples were whipped in modified 100 mL disposable cups (Sarstedt, Wexford, Ireland) that were pre-drilled with a 0.5 cm hole at the centre of the bottom of the cup. This hole was covered with duct tape for the whipping duration. After completion of whipping, the beaters were carefully removed from the foam to prevent foam damage. To compare cross-linking time, the microgel samples were whipped directly after $CaCl_2$ addition (0 h) or 24 h after addition. After foaming, samples were stored in closed containers at 4 °C.

2.9. Foam textural properties

Texture parameters of the samples were obtained using a texture analyser (TA.XT.plus, Texture Analyser, Stable Micro-systems, Godalming, UK). The method was followed as per Dabestani and Yeganehzad (2019) with slight modification. To prevent any edge effect, the foamed samples in 120 mm diameter containers were penetrated with an aluminium cylinder (36 × 36 mm) at a constant velocity of 1 mm s^{-1} for a distance of 10 mm. The force at target and the positive area of the curve were used as firmness and consistency, respectively. Foam texture was assessed immediately after foaming and after 6 months storage.

2.10. Foam characterisation

Immediately after whipping, the foam volume was read from the graduated scale on the container. After that, the duct tape was removed from the container and the container was placed over a beaker. The stability of the foam was measured by collecting the drained liquid in the beaker after 60 min. The drained liquid was collected via pipette for measurement. The following equations (Eqs. (1) and (2)) were used to measure foam overrun and stability respectively:

$$\text{Foam overrun (\%)} = (V1/V2) \times 100 \quad (1)$$

$$\text{Foam stability (\%)} = [(V2-V3)/V2] \times 100 \quad (2)$$

where V1 is the foam volume (mL) at 0 min, V2 is the volume of the initial liquid phase (mL) and V3 is the volume of liquid drainage (mL) after 60 min.

Maximum foam stability is 100%. Foam stability was also measured periodically over 2 years by monitoring drainage from the covered foams stored at 4 °C.

2.11. Analysis of foam structure

Foam bubble size was assessed using a light microscope equipped with a CCD camera (Olympus BX51 Microscope, Mason Technology, Dublin, Ireland). A drop of water was placed on a glass slide and a small amount of foam was transferred to this water droplet using a spatula. Singular bubbles that were not overlapping were analysed within 10 min after foaming. ImageJ software was used to determine bubble area (mm^2) and bubble wall thickness (mm) from at least 130 bubbles per sample.

Scanning electron microscopy was used to evaluate the micro-structure of WPI microgel foams using a method by Nooshkam, Varidi, and Alkobeisi (2022). Foams were frozen in liquid nitrogen and then freeze dried. The samples were mounted onto SEM specimen stubs and were sputter coated using an Emitech K550 gold sputter coater. SEM studies were carried out using a TM4000 SEM-EDX system (Hitachi Technologies) at 10 kV.

2.12. Statistical analysis

All experiments were carried out in triplicate and data were reported as mean ± standard deviation. Differences between means were evaluated by ANOVA using the Tukey posthoc test using Minitab statistical software version 18 (Minitab Inc., Pennsylvania, USA). Differences were considered significant if $P < 0.05$.

3. Results and discussion

3.1. Microgel fabrication

Microgels were formed following cross-linking for 24 h using a range of $CaCl_2$ concentrations (0.02, 0.05 or 0.1 M), as varying $CaCl_2$ concentration has been found to have different effects on whey protein aggregation and particle size (Beaulieu, Savoie, Paquin, & Subirade, 2002; Zhu & Damodaran, 1994a). It was found that the addition of $CaCl_2$ to the denatured WPI formed opaque solutions regardless of $CaCl_2$ concentration. The particle size was dependent on calcium concentration; as the calcium chloride concentration increased the particle size decreased (Table 1); however, 0.02 M $CaCl_2$ formed a continuous gel block rather than discrete particles, therefore particle size could not be measured. More available $CaCl_2$ could have led to higher aggregation activity of the unfolded interactive sites of whey protein leading to smaller, more tightly packed microgel particles. With less $CaCl_2$ present, it could be possible that unfolded loose strands of whey protein were not fully aggregated due to insufficient $CaCl_2$ to screen electrostatic repulsion, leading to fewer. Other studies have also found that the aggregation of WPI increased progressively with increased concentration of $CaCl_2$ and also the size of the particles decreased with increased calcium (Beaulieu et al., 2002; Zhu & Damodaran, 1994a).

The foaming properties of the microgels were tested 24 h after $CaCl_2$ addition. Samples were whipped for 5 or 10 min to establish if whipping time affected the overall foaming ability of the microgels. With increasing calcium concentration and increased whipping

Table 1
The effect of $CaCl_2$ concentration on particle size (μm) of whey protein microgel particles cross-linked for 24 h.[a]

Parameter	Value		
$CaCl_2$ (M)	0.02	0.05	0.1
D (3,2) (μm)	N/D	97.30 ± 0.13[a]	43.88 ± 2.46[b]

[a] Addition of 0.02 M $CaCl_2$ formed a macro-gel and could not be measured by the Mastersizer. Means with different letters indicate significant differences ($P < 0.05$).

time from 5 to 10 min, the foam overrun increased (Table 2). This could be due to the smaller particle size at higher ionic concentrations. The smaller particles could be more capable of adsorbing at the air/water interface than the larger microgels. Other studies have also found that the foamability of β-lactoglobulin (β-lg) microgels or whey protein fluid gels depended on particle size (Lazidis et al., 2016; Murphy, Farkas, & Jones, 2016; Rullier, Novales, & Axelos, 2008). The authors found that smaller protein particles could adsorb more quickly at the interface than larger particles facilitating foam formation. In addition, the microgels formed at lower ionic strength had higher viscosity values, which could have contributed to lower foam overrun. On addition of 0.02 M $CaCl_2$ the microgel sol viscosity was 7576 mPa, which decreased to 1659 mPa when 0.1 M $CaCl_2$ was added (Table 3). Increased viscosity minimises the incorporation of air into the system which leads to reduced foam overrun (Patino, Delgado, & Fernández, 1995). Tomczyńska-Mleko (2013) used a similar method to form aerated gels, however, differences occurred as the authors formed a semi-solid continuous gel with air bubbles present within the continuous gel. In this study, microgel solutions were formed whereby when whipped, the microgels resided in the continuous phase stabilising the air bubbles. Additionally, the concentrations used by Tomczyńska-Mleko (2013) are similar to the low concentration of 0.02 M used in this study which in both cases led to the formation of a continuous gel.

Addition of 0.1 M Ca^{2+} was chosen as the optimum concentration for microgel formation as foams with the greatest overrun and stability were formed. Microgels formed with 0.1 M Ca^{2+} are therefore used for the remainder of the study.

3.2. Native whey protein vs. whey protein microgel foaming

The foaming properties of microgels (cross-linked for 24 h) were compared with the foaming properties of native WPI. Foaming of native whey protein solutions were found to be significantly affected by whipping time. The highest overrun occurred with 5 min whipping (761%), but it decreased when whipping was carried out for 10 min (683%) (Table 2). The foam overrun of native WPI was significantly higher than the microgel foams regardless of whipping time (Table 2). Stability of the WPI foams was not significantly different between the two whipping times (94–98%), however, these foams slowly drained after the 60 min test time and foams typically collapsed within 2 h.

For the microgels, small amounts of liquid drainage did occur with stability values ranging from 88 to 93% regardless of the concentration of $CaCl_2$ added. Stability of foams formed from 0.02 M $CaCl_2$ microgels were significantly lower than WPI foam stability. However, after the 60 min test period no further liquid drained from these foams. The remaining foam remained stable without further drainage for an extended period of > 2 years. This was measured periodically over 2 years by monitoring drainage from the covered foams stored at 4 °C, and in that time period no drainage occurred, and the foams remained visually intact. Another study formed aerated gels, however, they were not as stable as air only remained within the gels for 41 days compared with 2 years in this study (Tomczyńska-Mleko, 2013).

The microgel foams were found to have lower overrun but better foam stability compared with foams produced using native whey protein. The difference in overrun could have occurred because of the ability of the native whey protein to adsorb at the air/water interface at a faster rate than microgels due to the smaller size and mobility of native proteins (Li et al., 2020a,b). Microgels at interfaces may take longer to adopt a favourable adsorption orientation compared with native WPI. Li et al. (2020a,b) found that egg white protein foams had higher overrun than those formed using egg white protein microgels due to the size differences between protein molecules and microgels. Zhu and Damodaran (1994b) also found that smaller monomeric whey proteins were more capable of producing foam with higher overrun, but the larger polymeric protein molecules contributed to foam stability. The monomeric species were capable of rapidly migrating, adsorbing, and unfolding at the air/water interface contributing to foam formation while the aggregated proteins increased the viscoelastic properties of the films leading to more stable foams (Rullier, Axelos, Langevin, & Novales, 2010; Rullier et al., 2008). Similarly Lazidis et al. (2016) found that their smaller protein particles could diffuse faster to the interface. The authors also found that their whey protein fluid gels could create the same amount of foam as native whey protein but with improved stability. The foam overrun of their native whey protein and whey protein fluid gels ranged from 197 to 240% (Lazidis et al., 2016). In this study, the WPI microgels foaming properties were greater as the microgel foams had significantly greater overrun (378%), while also providing excellent stability.

Viscosity is another factor that influences the whipping ability of the samples. As shown in Table 3, native WPI had a much lower viscosity compared with the microgels. The viscosity of the microgels was greater due to their aggregated cross-linked structure. The large disparity between the viscosity values correlates with the overrun results as more viscous systems minimise the incorporation of air into the solution leading to lower overrun values.

The storage and loss modulus of the microgels were greater than those of native WPI (Fig. 1). The protein solutions without Ca^{2+} remained in their native state where the protein molecules were flexible and free to move around displaying an entangled solution. However, with calcium addition to heat denatured WPI, much larger aggregates were present due to cross-linking of the protein molecules, and this contributed to a more interconnected elastic structure. The higher G′ values of the microgels indicated that heat denaturation followed by $CaCl_2$ addition induced gel formation of the protein solutions (Nicorescu et al., 2008). Whey protein microgels are not a build-up of simple polymer chains, but they

Table 2
Foam overrun (%) at 5 or 10 min whipping of native WPI and microgel particles cross-linked for 24 h.[a]

Sample	Overrun (%) at whipping time	
	5 min	10 min
Native WPI	761 ± 9.62^{aA}	683 ± 16.67^{aB}
Microgels formed with 0.02 M $CaCl_2$	189 ± 19.25^{cB}	289 ± 19.25^{cA}
Microgels formed with 0.05 M $CaCl_2$	283 ± 28.87^{bA}	317 ± 28.87^{cA}
Microgels formed with 0.1 M $CaCl_2$	306 ± 9.62^{bB}	378 ± 19.25^{bA}

[a] Means with lower case different letters within a column and data with upper case different letters within rows indicate significant differences ($P < 0.05$).

Table 3
Viscosity values of native WPI and microgels left to cross-link with $CaCl_2$ after 0 and 24 h.[a]

$CaCl_2$ (M)	Viscosity (mPa)	
	0 h	24 h
Native WPI	3.42 ± 0.10^{c}	N/D
0.02	181.42 ± 10.56^{a}	7576.32 ± 171.74^{a}
0.05	114.43 ± 3.35^{b}	3095.10 ± 253.80^{b}
0.1	108.83 ± 2.63^{b}	1659.26 ± 649.33^{b}

[a] Means with different letters within a column indicate significant differences ($P < 0.05$).

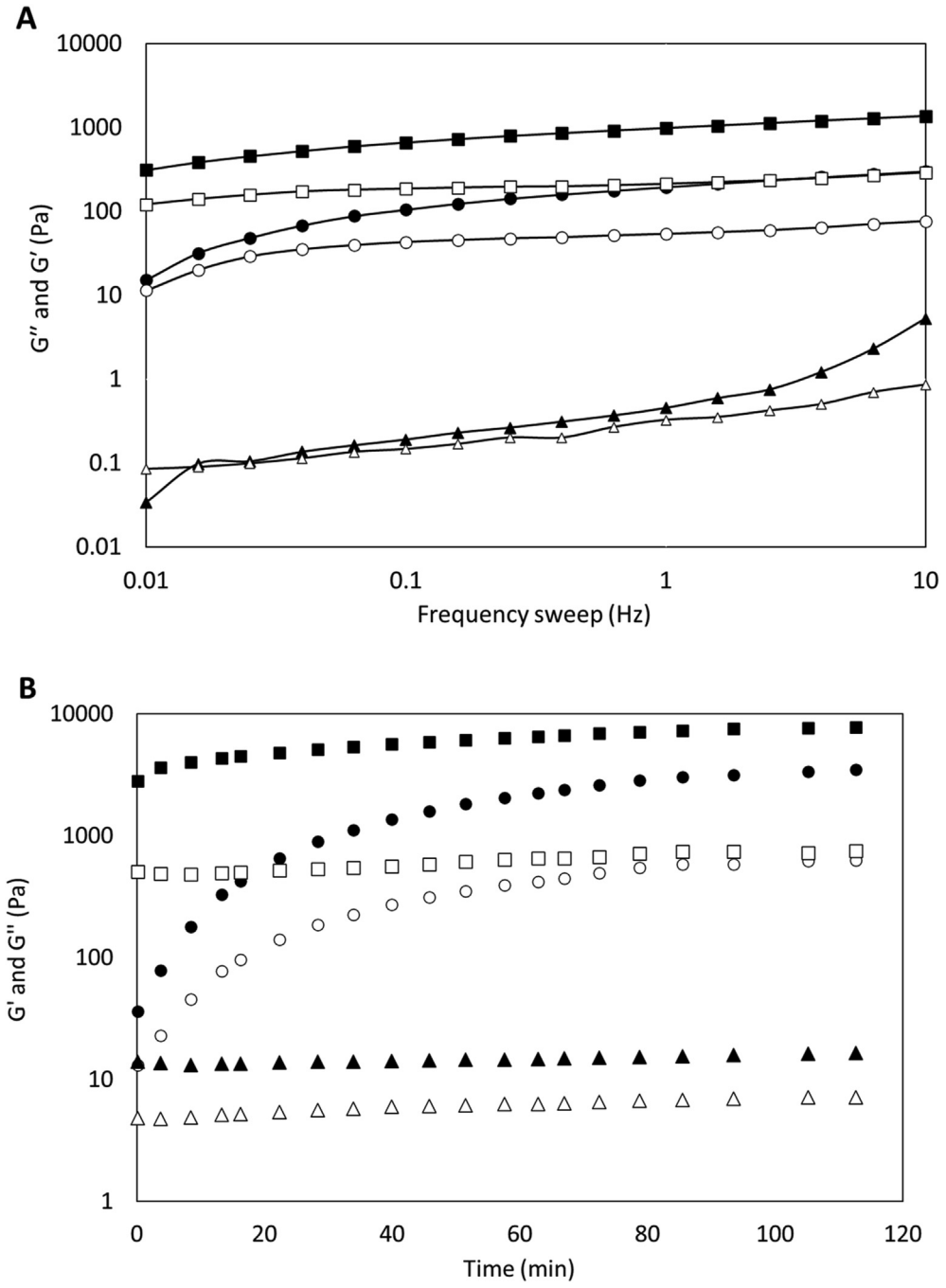

Fig. 1. Frequency sweep (A) and time sweep (B) for microgels formed using 0.1 M Ca^{2+} (0 h versus 24 h) and native WPI: ●, 0 h G′; ○, 0 h G″; ■, 24 h G′; □, 24 h G″; ▲, native WPI G′; △, G″.

possess a complex hierarchical structure that consists of clusters of aggregated denatured proteins (Schmitt et al., 2010). The stronger microgel sols could have resulted in more stable foams as increased elasticity has been found to aid with foam solidity and thus foam stability (Nicorescu et al., 2008; Rouimi, Schorsch, Valentini, & Vaslin, 2005).

The addition of $CaCl_2$ to heat denatured WPI improved the foam textural properties as both foam firmness and consistency increased (Table 4). The addition of $CaCl_2$ strengthened the protein bonds to form cross-linked gelled networks that, when whipped, led to the formation of stronger foams.

Image analysis of these foams indicated that the microstructure of the native whey protein and the microgel foams differed (Fig. 2). On a macroscopic level both foams appear similar, however, the bubbles were visibly larger in the native WPI foam (Fig. 2A,C). On a microscopic level, the native protein foam appeared as just bubbles surrounded by their liquid wall (Fig. 2B) while the microgel foams showed bubbles surrounded by cloudy gel-like white regions (Fig. 2D). The native protein foams had an average bubble area of 0.03 ± 0.02 mm^2 and a bubble wall thickness of 0.06 ± 0.02 mm. The bubble area or wall thickness could not be measured for the microgel stabilised foams as the presence of gel-like white regions

Table 4
Texture parameters of native WPI, 0.1 M Ca^{2+} microgel foams cross-linked for 0 and 24 h measured after manufacture and after 6 months storage.[a]

Sample	Firmness (N s^{-1})	Consistency (N s^{-1})
Native WPI	0.58 ± 0.05[d]	7.12 ± 0.31[d]
0 h cross-linked microgel foam	2.51 ± 0.20[c]	22.60 ± 2.31[c]
24 h cross-linked microgel foam	0.75 ± 0.06[d]	9.10 ± 0.75[d]
0 h cross-linked microgel foam stored for 6 months	6.58 ± 0.37[a]	46.10 ± 1.67[a]
24 h cross-linked microgel foam stored for 6 months	3.89 ± 0.33[b]	40.27 ± 0.82[b]

[a] Means with different letters within a column indicate significant differences ($P < 0.05$).

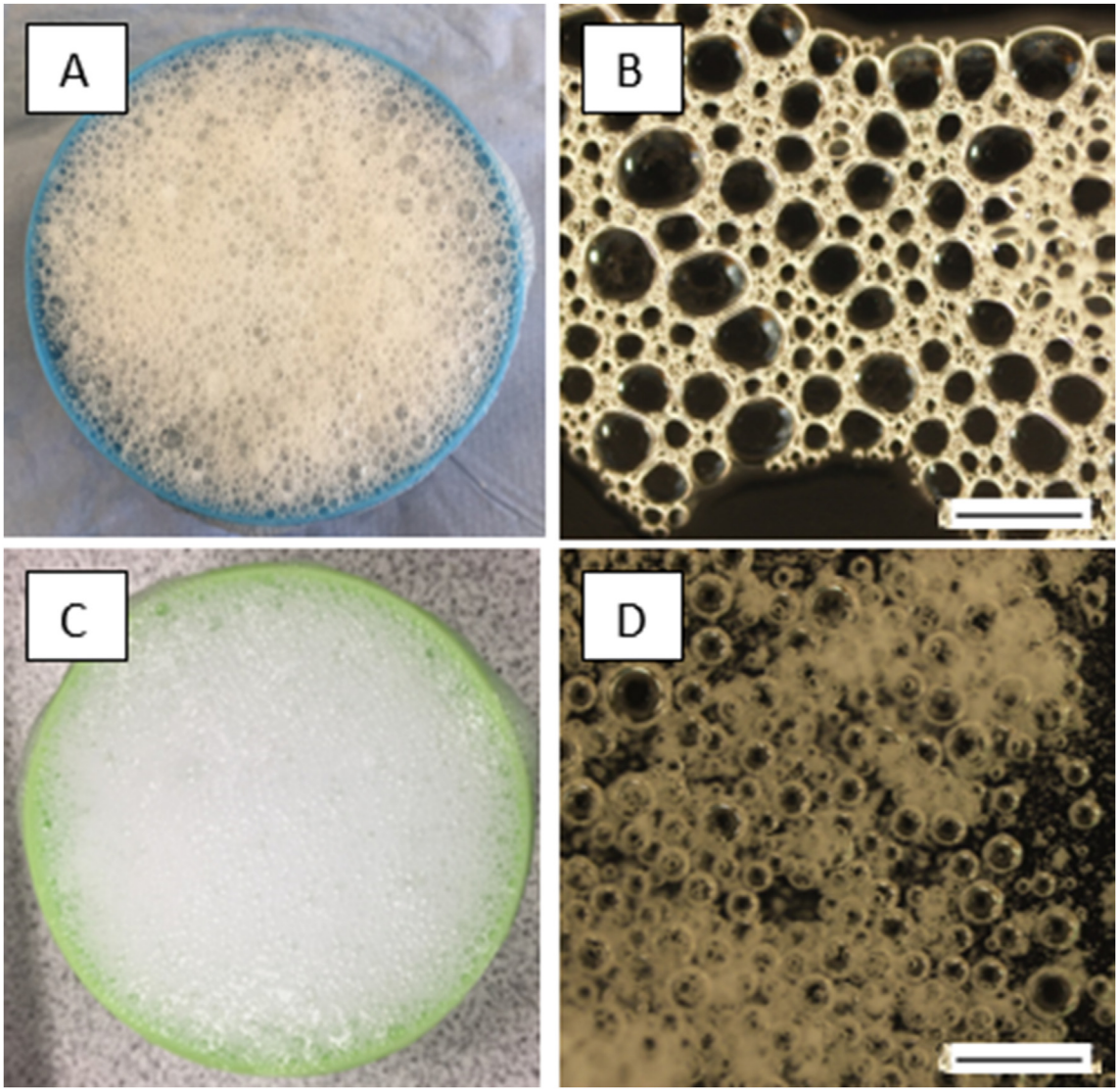

Fig. 2. Images of macroscopic foam (A) and a microscopic foam (B) of 10% WPI and of macroscopic (C) and microscopic (D) microgels formed using 0.1 M $CaCl_2$ and whipped. Scale bar represents 2 mm.

hindered the ability of the software to accurately measure these values as the white regions obstructed the bubbles. However, visually, it is evident that the bubbles in the microgel foams were smaller than those in the native whey protein foams. This difference in microstructure could potentially contribute to the extreme stabilising ability of microgels to form ultra-stable foams.

The presence of a gelled network amongst the bubbles could have reduced foam destabilisation by preventing gas diffusion between the air bubbles. The scanning electron microscopy images in Fig. 3 showed microstructures of a porous interconnected structure suggesting that the air bubbles were trapped and stabilised amongst a cohesive network formed by the microgels. Other studies have found that particles can remain in the liquid phase where they could act as corks and increase the viscosity thus, slowing down or eliminating drainage (Gharbi & Labbafi, 2019; Rullier et al., 2008).

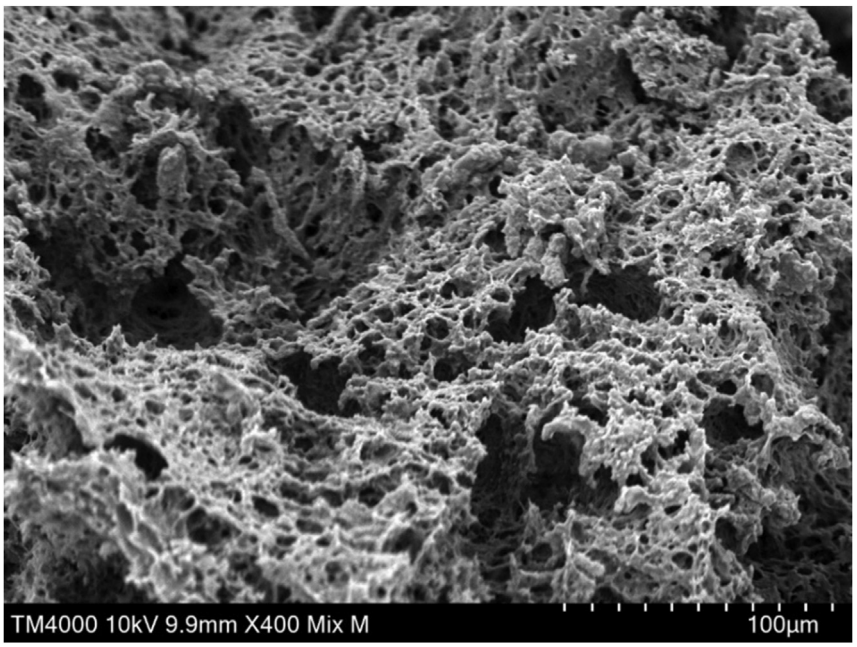

Fig. 3. Scanning electron microscopy image of WPI microgel foam.

3.3. Effect of cross-linking time on microgels

The effect of crosslinking time of the microgels rheological, textural, and foaming properties was investigated. As shown above, native WPI produced foams with high overrun but low stability, while the opposite occurred for the WPI microgels. Therefore, it was decided to examine foaming microgels immediately on Ca^{2+} addition (0.1 M) without any crosslinking time (0 h cross-linking) to see whether the foams could benefit from being simultaneously in their native denatured state while also forming cross-links upon $CaCl_2$ addition to produce foams with a combined functionality with greater overrun and stability.

Frequency and time sweeps of the microgels that were left to cross link for 0 and 24 h were compared (Fig. 1). Frequency sweeps are carried out to characterise biopolymer systems where entangled solutions, weak gels and strong gels can be identified (Garrec & Norton, 2012). The microgels were found to be marginally dependent on frequency, G′ and G″ increased slightly as the frequency increased from 0.01 to 10 Hz, and they were found to be more elastic than viscous (Fig. 1A). The storage and loss modulus of the microgels that were cross-linked for 24 h were considerably greater than those cross-linked for 0 h. This suggests that longer cross-linking allowed proteins more time to aggregate and become internally covalently cross-linked, leading to the formation of stronger microgels.

After $CaCl_2$ addition (0 h), G′ and G″ increased markedly until approximately 80 min, thereafter G′ and G″ plateaued (Fig. 1B). In comparison, the microgels cross-linked for 24 h showed slight increase in G′ and G″ before reaching a plateau. This suggested that on addition of $CaCl_2$ the denatured WPI formed microgels with increased structuring within the sample, whereas after 24 h there was little structuring occurring as the microgels were mostly formed. For both samples (0 h versus 24 h) the storage modulus was greater than the loss modulus which signifies typical features of an interconnected structure (Moakes, Sullo, & Norton, 2015).

Foam overrun values were considerably higher for foams cross-linked at 0 h compared with those cross-linked for 24 h regardless of Ca^{2+} concentration (Table 5). The stability of the 0 h cross-linked microgel foams was also greater (100%) as there was no drainage, whereas the microgels that were left to cross-link for 24 h had ~ 10% loss as liquid drained from the foams. The microgel foams remained stable for > 2 years forming ultra-stable foams.

Table 5
Overrun values of microgels that were left to cross-link with $CaCl_2$ for 0 h and 24 h.[a]

$CaCl_2$ (M)	Overrun (%)	
	0 h	24 h
0.02	683 ± 48.11[b]	289 ± 19.25[b]
0.05	717 ± 15.91[b]	317 ± 28.87[b]
0.1	756 ± 9.62[a]	378 ± 19.25[a]

[a] Means with different letters within a column indicate significant differences ($P < 0.05$).

The viscosity of the microgel sols measured directly after calcium addition was lower compared with those cross-linked for 24 h (Table 3). This lower viscosity coupled with weaker storage and loss moduli might have allowed more air to be incorporated into the system leading to greater foam formation while also allowing the microgels to adsorb at the air/water interface at a faster rate than the 24 h cross-linked microgels. Also, because the microgels cross-linked for 0 h were forming over time they could have been continually strengthening the foam leading to a more stable structure.

The textural parameters in Table 4 indicated that the 0 h cross-linked microgel foams were firmer and more consistent than foams formed from 24 h cross-linked microgels. Similar results were found by Nooshkam et al. (2022), whereby foams with the greatest overrun had greater texture parameters. However, the authors suggested that the air bubbles within the continuous phase acted as active filler particles, enhancing the strength of the foam as a consequence of their close packing and connection.

The texture of the microgel foams were also measured 6 months after formation. Foam firmness and consistency significantly increased regardless of cross-linking time; however, foams formed from 0 h cross-linked microgels had higher firmness and consistency after 6 months. Fig. 4 shows an image of foams made

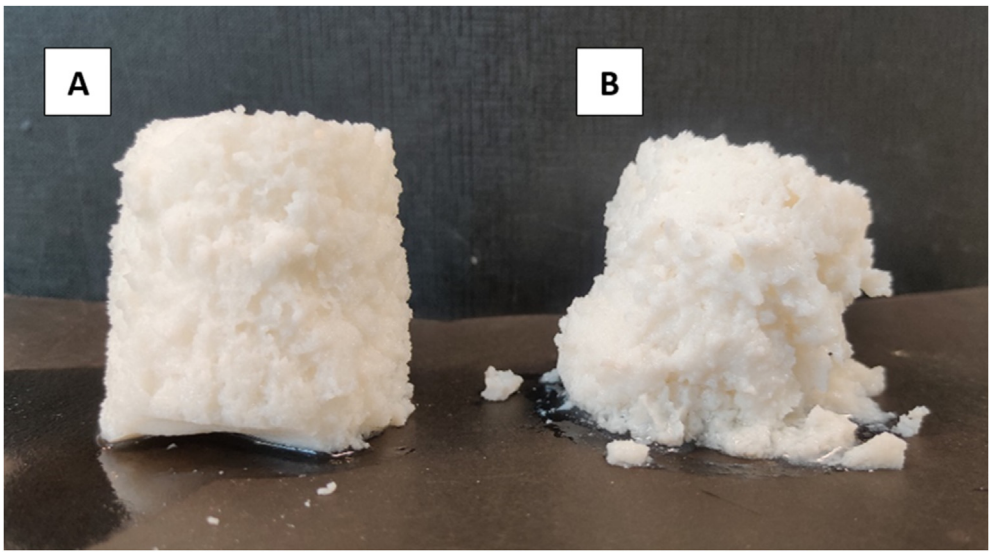

Fig. 4. Foams formed from microgels made using 0.1 M Ca^{2+} cross-linked for (A) 0 h and (B) 24 h. Image taken 6 months after foam production.

from 0 h and 24 h cross-linked microgels. The picture of the foams was taken 6 months after they were made. The 0 h cross-linked microgel foam held its shape better than the 24 h cross-linked microgel foam; however, both foams were very stable, displaying self-supporting structures. Foams stabilised by WPI microgels clearly show stability well in excess of food surfactants in aerated systems.

Texture analysis of the foams supports the stability results of the microgels cross-linked for 0 or 24 h. The foams formed from WPI whipped directly after $CaCl_2$ addition (0 h) had zero drainage and were found to be firmer and more consistent compared with the 24 h cross-linked microgel foams. The improved texture of the foams could have aided to prevent liquid drainage.

3.4. SDS-PAGE, free sulphydryl content and surface hydrophobicity

SDS-PAGE images of the samples are represented in Fig. 5. Whey protein heated to 80 °C was analysed to show the effect of heat on protein structural changes. Upon heating WPI to 80 °C and cross-linking for 0 and 24 h, the electrophoretic patterns under non-reducing conditions showed polymeric bands at the top of the gel which were unable to enter indicating that the molecular mass of the sample was >260 kDa. Monomeric bands corresponding to α-lactalbumin (α-la) (~14 kDa), β-lg (~18 kDa) and bovine serum albumin (BSA) (~66 kDa) were less evident than those found in native WPI, indicating that the monomeric proteins were polymerised into aggregates. Similar results have been found by Zhu and Damodaran (1994b) and Hongsprabhas and Barbut (1997) whereby heated whey protein molecules aggregated and could not enter the gel. There are differences between the 0 and 24 h cross-linked microgel bands, the monomeric bands of α-la and β-lg are less visible for the 24 h cross-linked gels indicating that more of the monomeric proteins were polymerised into microgels. It can also be seen that the 24 h cross-linked microgels could barely enter the gel indicating their larger size due to the longer cross-linking time for polymer network formation. Under reducing conditions in all lanes, the bands corresponding to the protein aggregates that were unable to enter the gel disappeared and instead there were strong distinct bands corresponding to α-la, β-lg and BSA. The electrophoretic patterns of the heated WPI and the microgels were indistinguishable from native WPI, indicating that the protein

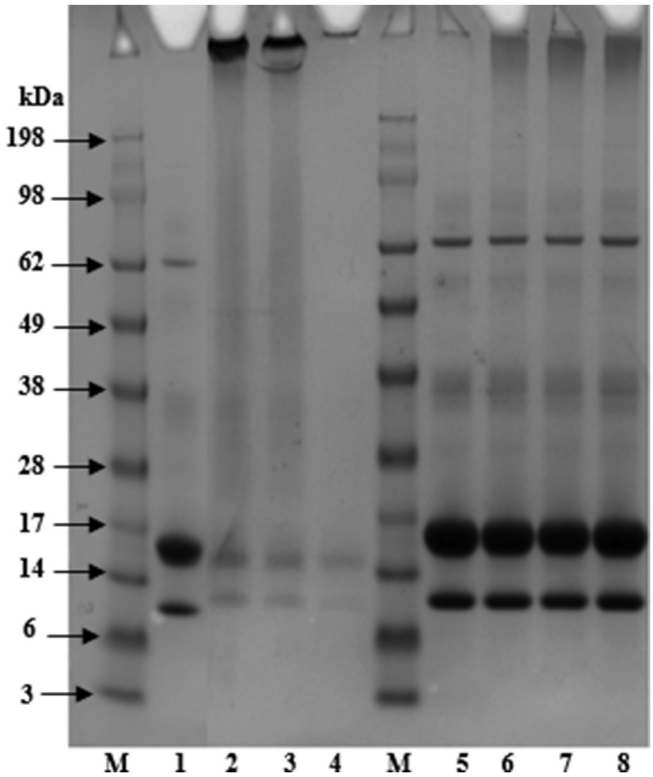

Fig. 5. SDS-polyacrylamide gel electrophoresis of WPI dispersions at 0.2%. Microgels are formed with 0.1 M Ca^{2+}. Lanes M represent the standard markers; lanes 1–4 are non-reduced and lanes 5–8 are reduced: lane 1, non-heated native WPI; lane 2, WPI heated to 80 °C; lane 3, 0 h cross-linked microgel; lane 4, 24 h cross-linked microgel; lane 5, nonheated native WPI; lane 6, WPI heated to 80 °C; lane 7, 0 h cross-linked microgel; lane 8, 24 h cross-linked microgel.

aggregates and microgels were formed via disulphide-sulphydryl interchange reactions (Davis & Foegeding, 2004).

The content of accessible sulphydryl groups increased when WPI was heated to 80 °C as a result of WPI unfolding and exposing buried sulphydryl groups (Table 6). The microgels cross-linked for 0 h had the highest free sulphydryl content (2.12 mM), which

Table 6
Protein hydrophobicity (H_0) and free sulphydryl (SH) content.[a]

Sample	H_0	Free SH (mM)
Native WPI	365.56 ± 17.97[b]	0.14 ± 0.06[d]
WPI at 80 °C	545.25 ± 12.86[a]	1.45 ± 0.25[b]
0 h cross-linked microgels	375.75 ± 4.14[b]	2.12 ± 0.12[a]
24 h cross-linked microgels	35.83 ± 2.03[c]	1.11 ± 0.00[c]

[a] Means with different letters within a column indicate significant differences ($P < 0.05$).

decreased to 1.11 mM when cross-linking time increased to 24 h indicating the formation of disulphide bonds. The SDS-PAGE data supports the free SH results in that the microgels were formed by disulphide bonds and that the disulphide bond content was greater for the 24 h cross-linked microgels.

The surface hydrophobicity of native WPI, heat denatured WPI, 0 h and 24 h cross-linked microgels are also shown in Table 6. Heat treatment of WPI to 80 °C for 30 min, exposed the hydrophobic regions of WPI. This was expected as heat treatment unfolds protein structures promoting hydrophobic interactions (Jia, You, Hu, Liu, & Xiong, 2015). On addition of $CaCl_2$ to heat denatured WPI, the surface hydrophobicity decreased. The addition of $CaCl_2$ screened the protein surface charges leading to protein aggregation and thus gel network formation which reduced the number of available binding sites for ANS (Liu et al., 2020; Schmitt, Bovay, Rouvet, Shojaei-Rami, & Kolodziejczyk, 2007). The microgels cross-linked for 24 h had significantly lower amount of exposed hydrophobic regions compared with the microgels cross-linked for 0 h. This suggests that the microgels were not fully formed on immediate addition of $CaCl_2$ indicating that the protein solution was not fully aggregated, whereas the microgels crosslinked for 24 h had more time to allow the protein molecules to crosslink forming more disulphide bonds, thus reducing surface hydrophobicity. The SDS-page also showed that crosslinking for 24 h led to larger protein aggregates, indicating that the microgels are made up of protein–protein hydrophobic interactions and covalent disulphide bonds.

4. Conclusion

Whey protein microgels produced via cold-set gelation showed foaming properties which were dependent on particle size, calcium concentration, cross-linking time, rheological properties, free sulphydryl and free surface hydrophobicity content. The microgels could form stable foams and image analysis indicated the ability of microgels to alter the microstructure of the bubbles in foams by creating an interconnected protein network stabilising the air bubbles. The strength of the microgels could be manipulated by altering the cross-linking time which in turn affected the foaming and textural properties. This can be used to create softer or more firm foams depending on the needs of the end product.

Foam overrun for microgel foams was lower than that of native protein foams; however, stability was greatly improved. The differing foaming abilities of native WPI and WPI microgels was due to differences in their rheological properties, which can be tailored by altering the $CaCl_2$ concentration or cross-linking time. Microgels can also alter the textural properties of foams, as both foam firmness and consistency were improved. This can be of use to the end user to tailor foods for specific needs such as low-calorie or high density foods.

This study demonstrated that the microgels had exceptional stabilisation ability, significantly beyond that of previously published work in the literature on microgel stabilised systems. The microgels decreased and even prevented liquid drainage, which led to the formation of ultra-stable foams remaining stable for > 2 years. The microgel properties can be manipulated by controlling particle size, $CaCl_2$ concentration, rheological and textural properties. The unique properties of microgel stabilised foams have much to offer in developing the science of food structuring and formulating novel and versatile structures to be used in the food industry. The WPI microgels can be used to prolong the lifetime of normally unstable foamed food products.

CRediT author statement

Jenna Lee: Conceptualization, Methodology, Validation, Formal analysis, Investigation, Writing – Original Draft, Visualization. **Elaine Duggan**: Resources, Writing – Review & Editing, Supervision, Project Administration, Funding acquisition, Visualization, Formal analysis.

Declaration of competing interest

The authors declare that they have no known competing financial interests or personal relationships that could have appeared to influence the work reported in this paper.

Acknowledgements

This project was funded by a grant (Project 15/F/737) administered by the Department of Agriculture, Food and the Marine (DAFM) of the Government of Ireland.

References

Abbasi, A., Emam-Djomeh, Z., Mousavi, M. A. E., & Davoodi, D. (2014). Stability of vitamin D3 encapsulated in nanoparticles of whey protein isolate. *Food Chemistry, 143*, 379–383.
Alavi, F., Tian, Z., Chen, L., & Emam-Djomeh, Z. (2020). Effect of $CaCl_2$ on the stability and rheological properties of foams and high-sugar aerated systems produced by preheated egg white protein. *Food Hydrocolloids, 106*. Article 105887.
Asghari, A. K., Norton, I., Mills, T., Sadd, P., & Spyropoulos, F. (2016). Interfacial and foaming characterisation of mixed protein-starch particle systems for food-foam applications. *Food Hydrocolloids, 53*, 311–319.
Bayram, T., Pekmez, M., Arda, N., & Yalçin, A. S. (2008). Antioxidant activity of whey protein fractions isolated by gel exclusion chromatography and protease treatment. *Talanta, 75*, 705–709.
Beaulieu, L., Savoie, L., Paquin, P., & Subirade, M. (2002). Elaboration and characterization of whey protein beads by an emulsification/cold gelation process: Application for the protection of retinol. *Biomacromolecules, 3*, 239–248.
Bryant, C. M., & McClements, D. J. (2000). Influence of xanthan gum on physical characteristics of heat-denatured whey protein solutions and gels. *Food Hydrocolloids, 14*, 383–390.
Cox, A. R., Aldred, D. L., & Russell, A. B. (2009). Exceptional stability of food foams using class II hydrophobin HFBII. *Food Hydrocolloids, 23*, 366–376.
Dabestani, M., & Yeganehzad, S. (2019). Effect of Persian gum and Xanthan gum on foaming properties and stability of pasteurized fresh egg white foam. *Food Hydrocolloids, 87*, 550–560.
Damodaran, S., Perkin, K. L., & Fennema, O. R. (2007). *Fennema's food chemistry* (4th ed.). Madison, Wisconsin, USA: CRC Press.
Davis, J. P., & Foegeding, E. A. (2004). Foaming and interfacial properties of polymerized whey protein isolate. *Journal of Food Science, 69*, C404–C410.
Dickinson, E. (2017). Biopolymer-based particles as stabilizing agents for emulsions and foams. *Food Hydrocolloids, 68*, 219–231.
Ellis, A. L., Mills, T. B., Norton, I. T., & Norton-Welch, A. B. (2019). The hydrophobic modification of kappa carrageenan microgel particles for the stabilisation of foams. *Journal of Colloid and Interface Science, 538*, 165–173.
Garrec, D. A., & Norton, I. T. (2012). Understanding fluid gel formation and properties. *Journal of Food Engineering, 112*, 175–182.
Gharbi, N., & Labbafi, M. (2019). Influence of treatment-induced modification of egg white proteins on foaming properties. *Food Hydrocolloids, 90*, 72–81.
Gill, H. S., & Cross, M. L. (2000). Anticancer properties of bovine milk. *British Journal of Nutrition, 84*, 161–166.
Hill, C., & Eastoe, J. (2017). Foams: From nature to industry. *Advances in Colloid and Interface Science, 247*, 496–513.
Hongsprabhas, P., & Barbut, S. (1997). Structure-forming processes in Ca^{2+}-induced whey protein isolate cold gelation. *International Dairy Journal, 7*, 827–834.
Jia, D., You, J., Hu, Y., Liu, R., & Xiong, S. (2015). Effect of $CaCl_2$ on denaturation and aggregation of silver carp myosin during setting. *Food Chemistry, 185*, 212–218.

Kuhn, K. R., Cavallieri, Â. L. F., & da Cunha, R. L. (2010). Cold-set whey protein gels induced by calcium or sodium salt addition. *International Journal of Food Science and Technology, 45*, 348–357.

Lam, S., Velikov, K. P., & Velev, O. D. (2014). Pickering stabilization of foams and emulsions with particles of biological origin. *Current Opinion in Colloid & Interface Science, 19*, 490–500.

Lazidis, A., Hancocks, R. D., Spyropoulos, F., Kreuß, M., Berrocal, R., & Norton, I. T. (2016). Whey protein fluid gels for the stabilisation of foams. *Food Hydrocolloids, 53*, 209–217.

Lee, J., & Duggan, E. (2022). Improved stability of vitamin D3 encapsulated in whey protein isolate microgels. *International Dairy Journal, 129*. Article 105351.

Li, J., Fu, J., Ma, Y., He, Y., Fu, R., Qayum, A., et al. (2022). Low temperature extrusion promotes transglutaminase cross-linking of whey protein isolate and enhances its emulsifying properties and water holding capacity. *Food Hydrocolloids, 125*. Article.

Li, X., Murray, B. S., Yang, Y., & Sarkar, A. (2020a). Egg white protein microgels as aqueous Pickering foam stabilizers : Bubble stability and interfacial properties. *Food Hydrocolloids, 98*. Article 105292.

Li, X., Yang, Y., Murray, B. S., & Sarkar, A. (2020b). Combination of egg white protein and microgels to stabilize foams: Impact of processing treatments. *Journal of Food Engineering, 275*. Article 109860.

Liu, Z., Liu, C., Sun, X., Zhang, S., Yuan, Y., Wang, D., et al. (2020). Fabrication and characterization of cold-gelation whey protein-chitosan complex hydrogels for the controlled release of curcumin. *Food Hydrocolloids, 103*. Article 105619.

Madadlou, A., Famelart, M. H., Pezennec, S., Rousseau, F., Floury, J., & Dupont, D. (2020). Interfacial and (emulsion) gel rheology of hydrophobised whey proteins. *International Dairy Journal, 100*. Article 104556.

Moakes, R. J. A., Sullo, A., & Norton, I. T. (2015). Preparation and characterisation of whey protein fluid gels: The effects of shear and thermal history. *Food Hydrocolloids, 45*, 227–235.

Murphy, R. W., Farkas, B. E., & Jones, O. G. (2016). Dynamic and viscoelastic interfacial behavior of β-lactoglobulin microgels of varying sizes at fluid interfaces. *Journal of Colloid and Interface Science, 466*, 12–19.

Nicorescu, I., Loisel, C., Vial, C., Riaublanc, A., Djelveh, G., Cuvelier, G., et al. (2008). Combined effect of dynamic heat treatment and ionic strength on the properties of whey protein foams – Part II. *Food Research International, 41*, 980–988.

Nooshkam, M., Varidi, M., & Alkobeisi, F. (2022). Bioactive food foams stabilized by licorice extract/whey protein isolate/sodium alginate ternary complexes. *Food Hydrocolloids, 126*. Article 107488.

Patino, J. M. R., Delgado, M. D. N., & Fernández, J. L. (1995). Stability and mechanical strength of aqueous foams containing food proteins. *Colloids and Surfaces A: Physicochemical and Engineering Aspects, 99*, 65–78.

Ron, N., Zimet, P., Bargarum, J., & Livney, Y. D. (2010). Beta-lactoglobulin-polysaccharide complexes as nanovehicles for hydrophobic nutraceuticals in non-fat foods and clear beverages. *International Dairy Journal, 20*, 686–693.

Rouimi, S., Schorsch, C., Valentini, C., & Vaslin, S. (2005). Foam stability and interfacial properties of milk protein-surfactant systems. *Food Hydrocolloids, 19*, 467–478.

Rullier, B., Axelos, M. A. V., Langevin, D., & Novales, B. (2010). β-Lactoglobulin aggregates in foam films: Effect of the concentration and size of the protein aggregates. *Journal of Colloid and Interface Science, 343*, 330–337.

Rullier, B., Novales, B., & Axelos, M. A. V. (2008). Effect of protein aggregates on foaming properties of β-lactoglobulin. *Colloids and Surfaces A: Physicochemical and Engineering Aspects, 330*, 96–102.

Schmitt, C., Bovay, C., Rouvet, M., Shojaei-Rami, S., & Kolodziejczyk, E. (2007). Whey protein soluble aggregates from heating with NaCl: Physicochemical, interfacial, and foaming properties. *Langmuir, 23*, 4155–4166.

Schmitt, V., Destribats, M., & Backov, R. (2014). Colloidal particles as liquid dispersion stabilizer: Pickering emulsions and materials thereof. *Comptes Rendus Physique, 15*, 761–774.

Schmitt, C., Moitzi, C., Bovay, C., Rouvet, M., Bovetto, L., Donato, L., et al. (2010). Internal structure and colloidal behaviour of covalent whey protein microgels obtained by heat treatment. *Soft Matter, 6*, 4876–4884.

Tan, Y., Liu, J., Zhou, H., Mundo, J. M., & McClements, D. J. (2019). Impact of an indigestible oil phase (mineral oil) on the bioaccessibility of vitamin D 3 encapsulated in whey protein-stabilized nanoemulsions. *Food Research International, 120*, 264–274.

Thermoscientific. (2020). *Ellman's reagent*. Thermo Fisher Scientific Inc., Rockford, IL, USA: https://assets.fishersci.com/TFS-Assets/LSG/manuals/MAN0011216_Ellmans_Reag_UG.pdf.

Tomczyńska-Mleko, M. (2013). Structure and stability of ion induced whey protein aerated gels. *Czech Journal of Food Sciences, 31*, 211–216.

Ustunol, Z. (2014). *Applied food protein chemistry* (1st edn.). Holboken, NJ, USA: Wiley-Blackwell.

Weigle, D. S., Breen, P. A., Matthys, C. C., Callahan, H. S., Meeuws, K. E., Burden, V. R., et al. (2005). A high-protein diet induces sustained reductions in appetite, ad libitum caloric intake, and body weight despite compensatory changes in diurnal plasma leptin and ghrelin concentrations. *American Journal of Clinical Nutrition, 82*, 41–48.

Zhu, H., & Damodaran, S. (1994a). Effects of calcium and magnesium ions on aggregation of whey protein isolate and its effect on foaming properties. *Journal of Agricultural and Food Chemistry, 42*, 856–862.

Zhu, H., & Damodaran, S. (1994b). Heat-induced conformational changes in whey protein isolate and its relation to foaming properties. *Journal of Agricultural and Food Chemistry, 42*, 846–855.